NACA

RESEARCH MEMORANDUM

EXPERIMENTAL INVESTIGATION OF EFFECT OF COOLING AIR ON TURBINE PERFORMANCE OF TWO TURBOJET ENGINES MODIFIED FOR AIR-COOLING

By Gordon T. Smith, John C. Freche, and Reeves P. Cochran

Lewis Flight Propulsion Laboratory
Cleveland, Ohio

NATIONAL ADVISORY COMMITTEE
FOR AERONAUTICS

WASHINGTON

January 25, 1956

NATIONAL ADVISORY COMMITTEE FOR AERONAUTICS

RESEARCH MEMORANDUM

EXPERIMENTAL INVESTIGATION OF EFFECT OF COOLING AIR ON TURBINE PERFORMANCE OF TWO TURBOJET ENGINES MODIFIED FOR AIR-COOLING

By Gordon T. Smith, John C. Freche, and Reeves P. Cochran

SUMMARY

An investigation was undertaken at sea-level static conditions to determine the effects of radial discharge of cooling air from turbine rotor blades on turbine performance in two turbojet engines, one with a centrifugal compressor and the other with an axial-flow compressor. Each engine was operated so that performance comparisons could be made between cooled- and uncooled-turbine data. During cooled operation, the cooling air was discharged radially into the gas stream from the rotor blade tips.

The efficiency (as defined herein) of neither turbine was seriously affected by tip discharge of cooling air at coolant- to gas-flow ratios below 0.03. It appeared that the work required to pump the cooling air through the rotor was partially regained.

INTRODUCTION

Air-cooling of turbine blades as a means of improving engine performance through increased turbine-inlet temperatures or of reducing turbine critical-material content has been investigated both experimentally and analytically in the past. In evaluating the desirability of such cooling, the effect of air-cooling on the performance of the engine and the principal engine components has also been investigated. Methods for determining performance characteristics are presented in reference 1. References 2 to 5 show analytically the performance gains possible with air-cooling. In addition, the reduction in critical-material content possible with turbine air-cooling is shown in reference 5. The effect of cooling on turbine efficiency is analytically predicted in reference 6. The results of experimental cold-air turbine tests in reference 7 indicate that a 1/2-percent reduction in turbine efficiency occurred with the use of a total coolant- to gas-flow ratio of 4 percent. The analytical results of reference 6 were predicated on

an increase in blade profile losses due to heat removal by the coolant; the experimental tests of reference 7 were obtained with no temperature difference between the main gas stream and the coolant.

The present investigation was undertaken at the NACA Lewis laboratory in order to explore the effect of radial discharge of cooling air from the blade tips on turbine performance at current operating temperatures. A centrifugal-compressor engine and an axial-flow-compressor engine were modified for air-cooling and operated at sea-level static conditions to provide a comparison of uncooled- and cooled-turbine efficiency over a range of turbine operating conditions. The centrifugal-compressor engine was operated over a range of equivalent turbine speeds from 93 to 102 percent of design (both cooled and uncooled) and coolant- to gas-flow ratios from 0 to 0.08. The axial-flow-compressor engine was investigated over a range of equivalent turbine speeds from 70 to 88 percent of design for coolant- to gas-flow ratios from 0 to about 0.10. The range of equivalent turbine speed for the axial-flow-compressor engine was limited because the noncritical material used in the rotor blades prevented uncooled operation at higher turbine-inlet temperatures.

SYMBOLS

A	area, sq ft
c_p	specific heat at constant pressure, Btu/(lb)($^\circ$R)
f/a	fuel-air ratio
g	acceleration due to gravity, 32.17 ft/sec^2
$\overline{H}$	lower heating value of fuel, 18,750 Btu/lb
h'	total enthalpy, Btu/lb
J	mechanical equivalent of heat, 778 ft-lb/Btu
M	Mach number
N	rotational speed, rpm
p	static pressure, lb/sq ft
p'	total pressure, lb/sq ft
R	gas constant, ft-lb/(lb)($^\circ$R)

r_t turbine tip radius, 1.083 ft for turbine A and 1.428 ft for turbine B

T' total temperature, $^{\circ}R$

T_o NACA standard sea-level temperature, 518.7° R

U wheel speed, ft/sec

V absolute combustion-gas velocity, ft/sec

w weight flow, lb/sec

γ ratio of specific heats

δ ratio of pressure to NACA standard sea-level pressure of 2116 lb/sq ft

η efficiency

θ ratio of temperature to NACA standard sea-level temperature of 518.7° R

ω angular velocity, 1/sec

Subscripts:

a cooling air

ac actual

B burner

b compressor bleed

C compressor

f fuel

g combustion gas

id ideal

m mixture of cooling air and combustion gas

o refers to zero cooling air or zero compressor-bleed-air conditions

r recirculating compressor secondary bleed air

[redacted]

s	nonrecirculating compressor secondary bleed air
T	turbine
t	turbine blade tip
u	whirl component
x	axial component
0-5	engine measuring stations (fig. 3)

GENERAL CONSIDERATIONS

The performance of an uncooled turbine is generally described by plotting the equivalent turbine work $\Delta h_T'/\theta_3$ against the equivalent speed - weight-flow parameter w_3N/δ_3. Lines of constant turbine pressure ratio p_3'/p_4', constant equivalent turbine speed $N/\sqrt{\theta_3}$, and constant turbine efficiency η_T appear as plotted parameters. If the turbine stator is choked over the entire range of turbine operation, the turbine equivalent weight flow $w_3\sqrt{\theta_3}/\delta_3$ is a constant, and the parameter w_3N/δ_3 can be replaced by the equivalent turbine speed $N/\sqrt{\theta_3}$. The definition of turbine efficiency,

$$\eta_t = \left(\frac{\Delta h_T'}{\theta_3}\right) \Bigg/ c_{p,3}\, T_0 \left[1 - \left(\frac{p_4'}{p_3'}\right)^{\frac{\gamma-1}{\gamma}}\right],$$

permits the elimination of one of the parameters, either η_T, $\Delta h_T'/\theta_3$, or p_3'/p_4'. The turbine performance can therefore be completely described as a relation of the three parameters, $\Delta h_T'/\theta_3$, $N/\sqrt{\theta_3}$, and η_T.

If the turbine is operated as a component of a turbojet engine with a fixed jet nozzle area, the equivalent engine speed $N/\sqrt{\theta_1}$ may be used as a parameter replacing any one of the turbine parameters just discussed; and the turbine performance may be described, for example, as a relation of the parameters $\Delta h_T'/\theta_3$, $N/\sqrt{\theta_3}$, and $N/\sqrt{\theta_1}$. If this turbine component is cooled by air flowing radially through the turbine rotor, the coolant flow ratio w_a/w_3 will determine the equivalent turbine speed required to produce a fixed value of $\Delta h_T'/\theta_3$ at a fixed engine speed of $N/\sqrt{\theta_1}$. Therefore, the coolant flow ratio must be employed as an additional parameter. Bleeding compressor-discharge air

in varying amounts has a similar effect, and the compressor bleed ratio w_b/w_3 must also be employed as a parameter to describe the turbine performance. For a particular turbine a relation of any three of the parameters, $\Delta h_T'/\theta_3$, η_T, $N/\sqrt{\theta_3}$, $N\sqrt{\theta_1}$, and w_a/w_3 or w_b/w_3, will determine the turbine operating conditions.

Data were obtained during this investigation by operating the engine with a fixed tail-pipe area at several constant values of equivalent engine speed. At each equivalent engine speed, $\Delta h_T'/\theta_3$ and $N/\sqrt{\theta_3}$ were varied by passing varying amounts of cooling air through the turbine, or by bleeding various amounts of air from the discharge of the engine compressor and removing it from the engine cycle. During the cooled runs, the work and inlet temperature changes caused by pumping different rates of cooling air through the rotor caused variations in the equivalent work and equivalent turbine speed. During uncooled operation, the work and temperature changes caused by varying loads imposed on the turbine by the engine compressor produced the variation in equivalent work and equivalent turbine speed.

The data were plotted as illustrated in figure 1 to permit a comparison of the cooled- and uncooled-turbine efficiencies at the same turbine map points. The three parameters, w_a/w_3 or w_b/w_3, $N/\sqrt{\theta_1}$, and $N/\sqrt{\theta_3}$, are shown in figure 1(a). (The turbine stator was choked over the entire range of these data.) Here w_a/w_3 and w_b/w_3 were each plotted against $N/\sqrt{\theta_3}$ for constant values of $N/\sqrt{\theta_1}$.

The three parameters, $\Delta h_T'/\theta_3$, $N/\sqrt{\theta_3}$, and $N/\sqrt{\theta_1}$, are shown in figure 1(b) with lines of constant w_a/w_3 or w_b/w_3 superimposed on the map by cross-plotting from figure 1(a). Figure 1(c) shows η_T, $N/\sqrt{\theta_3}$, and $N/\sqrt{\theta_1}$ with lines of constant w_a/w_3 or w_b/w_3 also cross-plotted from figure 1(a). (An efficiency ratio, rather than η_T, was used here for plotting convenience.) Figure 1(d) was obtained by cross-plotting lines of constant $\Delta h_T'/\theta_3$ from figure 1(b) on the coordinate system of figure 1(c). A composite of figure 1(d) for the cooled and uncooled operations describes the performance in terms of the parameters $\Delta h_T'/\theta_3$, $N/\sqrt{\theta_3}$, and $\eta_T/\eta_{T,o}$, thus permitting a comparison of the $\eta_T/\eta_{T,o}$ cooled with $\eta_T/\eta_{T,o}$ uncooled at the same values of $\Delta h_T'/\theta_3$ and $N/\sqrt{\theta_3}$.

The preceding treatment of the data assumes that the turbine efficiency is completely described by some function of the parameters

$N/\sqrt{\theta_3}$, $N/\sqrt{\theta_1}$, $\Delta h'_T/\theta_3$, and w_a/w_3 or w_b/w_3. Dimensional considerations indicate that the gas Reynolds number should be expected to affect the turbine efficiency. If the turbine rotor is cooled, reference 1 indicates that the coolant weight flow and the amount of heat transferred to the coolant in the rotor should be considered in addition to the gas Reynolds number. Reynolds number effects are often negligible over a wide range of Reynolds numbers, and the rotor heat-transfer rates involved in air-cooling of the rotor blades are small compared with the total heat content of the combustion gas. The data of this investigation were processed with the assumption that both Reynolds number and heat-transfer effects were small. Consequently, care must be exercised in extrapolating the results to materially different conditions of turbine operation.

Complications arise in defining and evaluating the efficiency of a cooled turbine. For example, there are two possible viewpoints regarding the working fluid in defining cooled-turbine efficiency. One is concerned with the combustion gas as the only working fluid, whereas the other is concerned with both combustion gas and cooling air as potential working fluids. Likewise the turbine output can be considered to be either the shaft work alone or the shaft work plus the work required to pump the cooling air through the rotor.

When all the factors discussed previously are considered, at least four possible definitions of turbine efficiency result:

$$\eta_T = \frac{w_1 \Delta h'_C}{w_3 \Delta h'_{g,T,id} + w_a \Delta h'_{a,T,id}} \tag{1}$$

$$\eta_T = \frac{w_1 \Delta h'_C + w_a \frac{U_t^2}{gJ}}{w_3 \Delta h'_{g,T,id} + w_a \Delta h'_{a,T,id}} \tag{2}$$

$$\eta_T = \frac{w_1 \Delta h'_C}{w_3 \Delta h'_{g,T,id}} \tag{3}$$

$$\eta_T = \frac{w_1 \Delta h'_C + w_a \frac{U_t^2}{gJ}}{w_3 \Delta h'_{g,T,id}} \tag{4}$$

where

$$\Delta h'_{g,T,id} = h'_3\left[1 - \left(\frac{p'_{4,m}}{p'_3}\right)^{\frac{\gamma-1}{\gamma}}\right]$$

and

$$\Delta h'_{a,T,id} = h'_5\left[1 - \left(\frac{p'_{4,m}}{p'_5}\right)^{\frac{\gamma-1}{\gamma}}\right]$$

Equations (1) and (2) consider both fluids entering the turbine as potential work sources. In addition, equation (2) includes the work required to pump the cooling air through the rotor as part of the turbine output. These definitions of efficiency are inconvenient to apply to cycle calculations, because the turbine cooling-air inlet total pressure p'_5 must be known, and the discharge pressure $p'_{4,m}$ does not depend solely on the combustion-gas conditions.

In equations (3) and (4), the combustion gas is the sole work source. Equation (3) is identical to the efficiency definition for an uncooled turbine, whereas equation (4) includes the pumping work in the turbine output. Equation (4) is used in the analysis of reference 5 to evaluate potentialities and limitations of turbine cooling. For the uncooled runs, the cooling air terms in all equations become zero, and the equations become the same as used for an uncooled turbine. The principal data presentation of the present report will utilize the efficiency definition of equation (4). A portion of the cooled-turbine data, calculated by each of the foregoing equations, is compared in order to illustrate the variation in the numerical values of efficiency with the definition employed.

APPARATUS AND INSTRUMENTATION

Turbines

Turbine A, installed in an engine having a double-entry centrifugal compressor, has 54 hollow, unshrouded blades incorporating twist and taper (fig. 2(a)). This turbine wheel is fully described in reference 8, and the turbine blades are discussed in reference 9. A standard turbine stator was used.

Turbine B, installed in an engine having a 12-stage axial-flow compressor, has 72 unshrouded, nontwisted, constant-chord blades with

corrugated inserts (fig. 2(b)). The mechanical design of the rotor and cooling-air supply system is discussed in reference 10. The aerodynamic design of the rotor and stator blades is described in reference 11. A special turbine stator with 64 solid, twisted blades was used with this rotor.

The rotor blade tip clearance (cold) was set for approximately 0.110 inch in both turbines. This tip-clearance value is within the limits normally specified for the standard production turbines of the engines used in this investigation. The tip radius was 1.083 feet for turbine A and 1.428 feet for turbine B.

Engine Installation

The installation of the centrifugal-compressor engine is illustrated in figure 3. A baffle wall that extended around the engine approximately at the burner inlets was used to prevent air in contact with hot parts of the engine from being drawn into the compressor inlet. The axial-flow-compressor engine installation was similar, except that no baffle wall was used.

On both engines, a number of bleed points at the compressor discharge were connected to a collecting manifold around the engine. The quantity of air flowing in the bleed system was remotely controlled by valves in the discharge lines. In the case of the centrifugal-compressor engine, these discharge lines emptied into the atmospheric sound-muffling chamber (fig. 3). On the axial-flow-compressor engine, the compressor-bleed discharge lines emptied into the test cell.

Measurements

The type and location of instruments at each instrumentation station are shown in figure 4(a) for the centrifugal-compressor engine and in figure 4(b) for the axial-flow-compressor engine.

In both installations, the engine-inlet air flow and the compressor-bleed air flow were measured by venturi tubes (figs. 3 and 4). The quantities of external cooling air were measured by standard flat-plate orifices upstream of the turbine cooling-air inlet. The axial-flow-compressor engine had overboard and interstage bleeds as integral engine functions. The air-flow quantities through these bleed lines were measured by sharp-edge orifices and pitot-static tubes as described in reference 10. In both engines fuel flow was measured by rotameters and engine speeds were measured by chronometric tachometers.

PROCEDURE

Engine Operation

Turbine A. - The centrifugal-compressor engine in which turbine A was installed was operated uncooled at equivalent engine speeds of 9325, 9715, 10,210, and 10,975 rpm. At each speed the compressor bleed was varied from zero to approximately 8 percent of the turbine-inlet mass flow. The compressor-bleed air was discharged to atmospheric pressure outside the sealed engine test cell. In order to maintain a constant equivalent engine speed $N/\sqrt{\theta_1}$, it was necessary to increase the turbine-inlet temperature, because the turbine specific work increased when air was bled from the compressor. As a result, the equivalent turbine speed $N/\sqrt{\theta_3}$ decreased, and the turbine operated in a region to the left of its normal operating line (fig. 1(b)).

Cooled-turbine operation was conducted at equivalent engine speeds of 9610, 10,145, 10,315, 10,785, and 10,890 rpm. Compressor air was not bled from the engine during these runs. Instead, cooling air was supplied to the rotor blades from a laboratory air system in quantities ranging from zero to approximately 8 percent of the turbine-inlet mass flow at each speed. Such operation also resulted in a reduction in the equivalent turbine speed due to the increase in turbine-inlet temperature associated with the increase in pumping work expended on the cooling air in the turbine rotor. Again, operation in a map region to the left of the normal turbine operating line resulted.

Turbine B. - The axial-flow compressor engine in which turbine B was installed was operated uncooled at equivalent engine speeds of 4990, 5485, and 5985 rpm. The compressor bleed was varied from zero to approximately 5 percent of the turbine-inlet mass flow during each run, and the bleed air was discharged into the test cell.

Cooled operation was conducted at equivalent engine speeds of 4995, 5490, and 5995 rpm. The cooling-air-flow rates were varied at each speed from zero to respective maximums of 11, 7, and 6 percent of the turbine-inlet mass flow. The operational characteristics of this turbine were similar to those of turbine A, and partial turbine maps were constructed as described previously.

Calculations

The calculation procedures employed to process both sets of turbine data were the same. Secondary-bleed-air terms that appear in the following equations were zero for turbine A. The enthalpy terms appearing as known quantities in subsequent energy balances were evaluated from directly measured temperatures and the charts of reference 12.

Flow rates. - The flow rates w_1, w_s, w_b, w_a, and w_f were determined from the calibrated instrumentation mentioned in the APPARATUS AND INSTRUMENTATION section. Other required flow rates and fuel-air ratios were computed from the following expressions:

$$w_2 = w_1 - w_b - w_s - w_r$$

$$w_3 = w_2 + w_f$$

$$w_{4,m} = w_3 + w_a + w_s$$

$$(f/a)_3 = w_f/w_2$$

$$(f/a)_4 = w_f/(w_2 + w_a + w_s)$$

Turbine-inlet conditions. - The turbine-inlet total pressure was determined from direct measurements upstream of the turbine stators. The turbine-inlet total temperature T'_3 was determined from an energy balance across the combustor that was solved for total specific inlet enthalpy h'_3:

$$h'_3 = \frac{w_2 h'_2 + w_f \eta_B \overline{H}}{w_3} \tag{5}$$

where η_B is 0.95 (based on combustor data) for the centrifugal-compressor engine and 0.98 (based on combustor data) for the axial-flow-compressor engine. Then T'_3 was determined from the charts of reference 12 and the calculated values of h'_3 and $(f/a)_3$.

Turbine-outlet conditions. - The static pressure downstream of the turbine exit was determined by a direct measurement from wall taps. The flow area was established before operation by measurement of the tail-cone geometry. The turbine-outlet temperature $T'_{4,m}$ was found from an energy balance across the turbine as indicated in sketch (a) and equation (6):

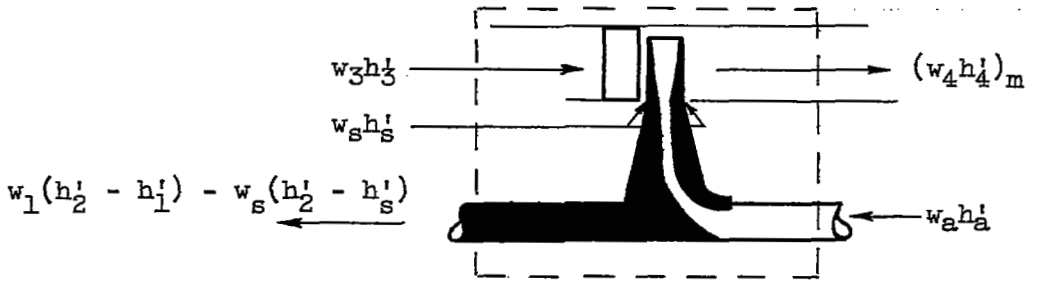

Sketch (a)

$$w_3h'_3 + w_ah'_a + w_sh'_s = w_1(h'_2 - h'_1) - w_s(h'_2 - h'_s) + (w_4h'_4)_m \qquad (6)$$

The term $w_r(h'_2 - h'_r)$ does not appear in equation (6) because $h'_2 = h'_r$. This energy balance was solved for $h'_{4,m}$; $T'_{4,m}$ was determined from $(f/a)_4$, $h'_{4,m}$, and the charts of reference 12.

With the assumption that $T'_{4,m} = T'_{4,x,m}$, the axial component of the total pressure was established by simultaneously solving the two following equations:

$$\left(\frac{p'_{4,x}}{p_4}\right)_m = \left[\left(1 + \frac{\gamma_4 - 1}{2} M_{4,x}^2\right)^{\frac{\gamma_4}{\gamma_4 - 1}}\right]_m \qquad (7)$$

and

$$w_{4,m} = A_4\left[p_4 M_{4,x}\sqrt{\frac{\gamma_4 g}{R_4 T'_4}}\left(1 + \frac{\gamma_4 - 1}{2} M_{4,x}^2\right)^{1/2}\right]_m \qquad (8)$$

For the centrifugal-compressor engine the area A_4 in equation (8) was the annular cross-sectional area at station 4. For the axial-flow-compressor engine A_4 was the area between the inner and outer surfaces of the tail cone. Inasmuch as these latter were surfaces of cones with different cone angles, the distance between the tail-cone surfaces was taken along a line normal to a mean line through the tail-cone gas passage.

When the value of $p'_{4,x,m}$ was found, it was then possible to compute $p'_3/p'_{4,x,m}$.

Turbine operational parameters. - The calculations of w_a/w_3 and w_b/w_3 were made directly from the quantities already discussed. The turbine speed N was determined from an engine measurement and $N/\sqrt{\theta_3}$ computed after obtaining T'_3. Calculation of the turbine specific output $\Delta h'_{T,ac}$ depends on which viewpoint is taken regarding the turbine output (GENERAL CONSIDERATION section). For the principal data presentation of this report, the cooling-air pumping work is regarded as part of the turbine work output. On this basis the turbine specific work output is expressed by the following relation:

$$\Delta h'_{T,ac} = \frac{w_1(h'_2 - h'_1) - w_s(h'_2 - h'_s) + w_a \frac{\omega^2 r_t^2}{gJ}}{w_3} = \frac{w_1 \Delta h'_C + w_a \frac{U_t^2}{gJ}}{w_3} \tag{9a}$$

The equivalent work $\Delta h'_{T,ac}/\theta_3$ was then computed directly.

When the pumping work is not assumed a part of the work output this expression reduces to

$$\Delta h'_{T,ac} = \frac{w_1(h'_2 - h'_1) - w_s(h'_2 - h'_s)}{w_3} = \frac{w_1 \Delta h'_C}{w_3} \tag{9b}$$

The ideal work can also be computed in two ways. Assuming that the combustion gas is the only working fluid, the total ideal turbine work can be expressed as

$$w_3 \Delta h'_{g,T,id} = w_3(h'_3 - h'_{4,g,id}) \tag{10}$$

where $h'_{4,g,id}$ is determined from the turbine pressure ratio $p'_3/p'_{4,x,m}$, $(f/a)_4$, and the charts and method of reference 12. Assuming the cooling air is also a working fluid and taking the work potential of the flow into account give

$$w_3 \Delta h'_{g,T,id} + w_a \Delta h'_{a,T,id} = w_3(h'_3 - h'_{4,g,id}) + w_a(h'_5 - h'_{4,a,id})$$

where, as before, $h'_{4,a,id}$ was determined from the charts and the pressure ratio $p'_5/p'_{4,x,m}$. The total pressure p'_5 was a directly measured quantity at the turbine rotor hub.

The various turbine efficiencies mentioned in the GENERAL CONSIDERATION section could then be computed.

RESULTS AND DISCUSSION

Performance Characteristics

Turbine A. - The turbine operating lines for constant equivalent engine speeds are presented on equivalent turbine work and equivalent turbine speed coordinate systems in figure 5 for turbine A. The data for uncooled operation (fig. 5(a)) exhibit virtually no change in equivalent turbine work as the compressor-bleed ratio is increased and as the equivalent turbine speed decreases. The zero coolant flow and the zero compressor-bleed lines in figure 5(a) and (b) were established by passing a mean line through all available zero flow data as shown in figure 6. During cooled operation as the coolant- gas-flow ratio increased the equivalent work increased substantially except along the maximum-engine-speed operating line, where it was essentially constant.

An increase in either compressor-bleed or coolant-flow ratio required a greater extraction of work per pound from the combustion gas. For the compressor-bleed runs, the additional work was expended in compressing the air prior to bleeding from the compressor discharge. For the cooled runs this additional work was expended in pumping the coolant through the turbine rotor.

The variation of the turbine-efficiency ratio with the equivalent turbine speed is shown in figure 7. The turbine efficiency used was that defined by equation (4). The turbine-efficiency ratio is the ratio of the turbine efficiency at a given condition to the turbine efficiency at zero coolant flow and zero bleed at the same equivalent engine speed. The turbine efficiency at zero coolant flow and zero bleed was 80 percent (± 1) over the range of equivalent turbine speeds investigated. At lower values of equivalent turbine speed during compressor-bleed (uncooled) operation (fig. 7(a)), the efficiency ratio decreased with decreasing equivalent turbine speed along a line of constant equivalent engine speed. Along the operating line for an equivalent engine speed of 9325 rpm, for example, the turbine efficiency decreased about 2 percent. For highest equivalent engine speed (10,975 rpm), the turbine-efficiency ratio was essentially constant.

During cooled operation the turbine-efficiency ratio increased as the coolant-flow ratio was increased (fig. 7(b)). The efficiency-ratio increase averaged about 6.5 percent for the maximum coolant-flow ratio of 0.08 considered over the range of equivalent turbine speeds investigated (93 to 102 percent of design).

The efficiency ratios (as determined by eq. (4)) for both cooled- and uncooled-engine operating data at the same values of equivalent turbine work and equivalent turbine speeds are compared in figure 8. The constant-equivalent-work lines for uncooled operation were extrapolated to cover the same speed range as covered by the data for cooled operation. At an equivalent turbine work of 19 Btu per pound and an equivalent turbine speed of 5340 rpm, figure 8 indicates that the turbine-efficiency ratio was decreased about $2\frac{1}{2}$ percent from the zero-bleed - zero-coolant - flow efficiency. The cooled-turbine-efficiency ratio at a coolant-flow ratio of 0.08 increased about $6\frac{1}{2}$ percent from the same point. Near design turbine speed this spread between the cooled- and uncooled-turbine-efficiency was less pronounced.

Turbine B. - The variation of equivalent turbine work with equivalent turbine speed for turbine B is illustrated in figure 9. The turbine design speed was not attained for the reason noted previously. For both uncooled (fig. 9(a)) and cooled (fig. 9(b)) operation, the equivalent work remained essentially constant for a given value of equivalent engine speed throughout the range of equivalent turbine speeds and bleed- or coolant-flow ratios investigated.

Variation of turbine-efficiency ratio with equivalent turbine speed is shown in figure 10. For zero coolant flow the turbine efficiency was about 67 to 72 percent over the range of equivalent turbine speeds investigated. The data trends were similar to those obtained with turbine A, although the magnitudes of the efficiency ratio changes were not as great. During uncooled operation the efficiency ratio decreased slightly (1/2 to 1 percent) with decreasing equivalent turbine speed along the lines of constant equivalent engine speed.

During cooled operation a slight increase in turbine-efficiency ratio occurred as the coolant-flow ratio was increased. The maximum increase was about 2 percent for a coolant-flow ratio of 0.07, compared with about 6 percent for a similar coolant-flow ratio with turbine A (fig. 7(b)).

A direct comparison of turbine efficiency ratios obtained by equation (4) for both cooled and uncooled operating data at the same equivalent work and equivalent turbine speed is shown in figure 11. At the lowest value of equivalent work considered, 14 Btu per pound, and an equivalent turbine speed of 2810 rpm (71 percent of design), the turbine-efficiency ratio decreased about 1/2 percent from the efficiency at the zero-bleed - zero-coolant - flow condition. The turbine-efficiency ratio at a coolant - to gas-flow ratio of 0.07 increased about 2 percent from the same point. This represents a total spread of $2\frac{1}{2}$ percent. Similar comparisons can be made at higher values of equivalent turbine speed.

Efficiency Comparisons

The cooled data obtained with each turbine were calculated to determine efficiencies as defined by equations (1) to (4). The variation of these efficiencies with equivalent turbine speed for a representative value of constant equivalent engine speed is shown in figure 12 for each turbine. Figure 13 shows a comparison of turbine-efficiency ratios for cooled and uncooled operation of turbine A where the efficiency is defined by both equations (3) and (4).

Comparison at representative equivalent engine speed. - Equations (1) and (2) (broken lines on fig. 12(a)) account for the extra energy supplied to the turbine system from the external air source and incorporate the internal pumping efficiency of the turbine rotor into an over-all efficiency definition. Comparisons between equations (1) and (3) and between equations (2) and (4) (fig. 12 (a)) show that this extra energy added to the system had little effect (a maximum of approximately $1\frac{1}{2}$ points) on the turbine efficiency. The largest difference (approximately $6\frac{1}{2}$ points) in efficiency occurs when equations (1) and (2) or equations (3) and (4) are compared. This indicates that inclusion of the cooling-air pumping work results in distinctly higher efficiencies, regardless of whether or not the cooling air is considered as a working fluid. The turbine efficiencies based on the assumption that the turbine output is the net shaft power delivered to the compressor (eqs. (3) and (1)) show a maximum decrease of about $1\frac{1}{2}$ and $2\frac{1}{2}$ points, respectively, ($N/\sqrt{\theta_3}$ = 5633, fig. 12(a)) from the turbine efficiency at the zero-coolant-flow operating point ($N/\sqrt{\theta_3}$ = 5768, fig. 12(a)). Turbine data obtained at zero coolant flow and zero bleed indicated that approximately 1 point of this reduction in efficiency was due to changes in turbine operating conditions. The net efficiency decrease due to the presence of cooling air (0.065 coolant-flow ratio) is therefore $\frac{1}{2}$ to $1\frac{1}{2}$ points. Had the efficiency as calculated by equations (1) and (3) exhibited the same 1-percent decrease as the efficiency of the uncooled turbine, the pumping work expended on the cooling air would have been completely regained by the turbine. Since this condition was closely approached, apparently a large part of the cooling-air pumping work was regained. A net increase of about 3 to 4 points occurs at a coolant-flow ratio of 0.065 when the rotor cooling-air pumping work is considered as part of the turbine output (eqs. (2) and (4)) and the decrease in the uncooled turbine efficiency is considered.

The broken lines fall above the solid lines at the higher values of equivalent turbine speed in figure 12. This occurs when the pumping action of the turbine rotor develops a pressure rise. The ideal work

of the cooling air then becomes negative and decreases the total available turbine ideal work. This decrease is the amount of work required to isentropically increase the cooling-air total pressure from the level at the rotor hub inlet to the total pressure of the cooling air and gas mixture at the turbine exit.

The efficiency curves for turbine B (fig. 12(b)) exhibit the same general behavior as the curves for turbine A, except that the trends are less pronounced. From figure 12 it is apparent that the efficiency (as defined herein) of neither turbine was seriously affected by tip discharge of cooling air at coolant-to-gas-flow ratios below 0.03. At the other equivalent engine speeds considered, the results were similar.

Comparison over range of equivalent engine speeds. - To illustrate efficiency comparisons over the entire speed range investigated, figure 13 presents turbine-efficiency ratios for cooled and uncooled operation for turbine A where the efficiency is defined by both equations (3) and (4). Figure 13(a) is the same as figure 8. It is repeated here for convenience in comparing with the curves for equation (3). In figure 13(b) it was not necessary to extrapolate the lines of constant equivalent turbine work for uncooled operation as was done in figure 13(a). It has been pointed out (fig. 12(a)) that the exclusion of pumping work made the largest change in the values of turbine efficiency defined by equations (1) to (4). The efficiency definition of equation (3) was chosen for this comparison because it differs from the definition of equation (4) only by the quantity of the pumping work.

As can be seen from figure 13(b), the turbine-efficiency ratio for cooled operation as defined by equation (3) falls below the efficiency ratio for uncooled operation. This is in contrast to the trend of turbine-efficiency ratio as defined by equation (4) (fig. 13(a)). However, even with the definition of equation (3) (which considers net shaft work as the total turbine work), turbine efficiency is not seriously affected by the radial discharge of cooling air at the tips of the turbine rotor blades. For example, at constant equivalent work and constant equivalent turbine speed, a maximum decrease in efficiency ratio of about 1 percent from the uncooled operation occurred with a coolant-flow ratio of 0.08.

Interpretation of Results

Possible mechanisms for explaining the behavior of efficiency with changes in rotor cooling-air flow are presented herein, and these data are compared with the results of other investigations.

The cooling-air pumping work is actually work that must be accomplished by the turbine. The turbine-efficiency definitions of

equations (2) and (4) take this into account. As noted before for turbine A, these efficiencies exhibit an increase as the cooling-air flow is increased. The discharge of blade cooling air at the blade tips with its resultant blockage and the effects of redistribution of combustion-gas flow may be of such a nature as to cause an improvement in the blade aerodynamic efficiency. However, large increases in efficiency would certainly not be expected if the rotor were well designed. The efficiency changes occurring with turbine A suggest that some additional effect may be present.

The following mechanism might be constructed. As the cooling air enters the turbine rotor stage at the blade tips, its whirl velocity is essentially the tip velocity of the turbine rotor. If the cooling air leaves the turbine stage without a change in this whirl velocity, it will not do work on the blades. If, on the other hand, cooling air is accelerated with the combustion-gas stream by virtue of its own energy, so that it is discharged with the same exit whirl as the combustion gas, the cooling air experiences a change in tangential momentum of $(w_a/g)(U_t - V_{u,4})$. With this momentum change, the cooling air would contribute an amount of work equivalent to $(w_a U_t/gJ)(U_t - V_{u,4})$. Actually, the acceleration of cooling air to combustion-gas velocity is probably incomplete, and the exit direction of the combustion-gas stream may be changed as a result of mixing. Some cooling air undoubtedly moves radially inward from the blade tip before leaving the stage. Consequently, the term $w_a U_t(U_t - V_{u,4})/gJ$ probably represent about the maximum work recoverable from the rotor blade cooling air. The increase in turbine efficiency (eq. (4)) with the addition of cooling air appears to indicate that at least a portion of this work is being realized.

The analysis of reference 6, which predicts an efficiency decrease with the addition of rotor blade cooling, does not consider the introduction of the coolant into the main gas stream. The reference assumes that blade cooling increases the blade profile losses as a result of the removal of heat from the rotor blade channel. Since the effect of cooling is confined to the two-dimensional losses (profile losses) in the rotor, the analysis cannot be expected to predict experimental trends when the flow pattern is distorted by cooling air discharged at the blade tips. Results of the present investigation interpreted on the basis of reference 6 indicate that blade profile losses due to air cooling are small compared with the effects of flow redistribution and cooling-air impulse.

CONCLUSIONS

An investigation was made at sea-level static conditions to determine the effect of radial discharge of cooling air from the rotor blade

tips on turbine performance in two turbojet engines. The efficiency (as defined herein) of neither turbine was seriously affected by tip discharge of cooling air at coolant- to gas-flow ratios below 0.03. The work required to pump the cooling air through the turbine rotors appeared to have been partially regained.

Lewis Flight Propulsion Laboratory
National Advisory Committee for Aeronautics
Cleveland, Ohio, October 25, 1955

3839

REFERENCES

1. Ellerbrock, Herman H., Jr., and Ziemer, Robert R.: Preliminary Analysis of Problem of Determining Experimental Performance of Air-Cooled Turbine. III - Methods for Determining Power and Efficiency. NACA RM E50E18, 1950.

2. Esgar, Jack B., and Ziemer, Robert R.: Review of Status, Methods, and Potentials of Gas-Turbine Air-Cooling. NACA RM E54I23, 1955.

3. Rossbach, Richard J., Schramm, Wilson B., and Hubbartt, James E.: Analysis of Factors Affecting Selection and Design of Air-Cooled Single-Stage Turbines for Turbojet Engines. I - Turbine Performance and Engine Weight-Flow Capacity. NACA RM E54C22, 1954.

4. Hubbartt, James E., Rossbach, Richard J., and Schramm, Wilson B.: Analysis of Factors Affecting Selection and Design of Air-Cooled Single-Stage Turbines for Turbojet Engines. III - Engine Design-Point Performance. NACA RM E54F16a, 1954.

5. Schramm, Wilson B., Nachtigall, Alfred J., and Arne, Vernon L.: Preliminary Analysis of Effects of Air Cooling Turbine Blades on Turbojet-Engine Performance. NACA RM E50E22, 1950.

6. Hawthorne, W. R., and Walker, Antonia B.: The Effect of Blade Cooling on Stage Efficiency of a Gas Turbine. Rep. No. 6574-2, Gas Turbine Lab., M.I.T., Mar. 15, 1949. (ONR Contract N5ori-78, Task Order 21, NR-220-010, Proj. DIC 6574.)

7. Ainley, D. G.: An Experimental Single-Stage Air-Cooled Turbine. Pt. II - Research on the Performance of a Type of Internally-Air-Cooled Turbine Blade. Aircraft Eng., vol. XXV, no. 295, Sept. 1953, pp. 269-276.

[redacted]

8. Schramm, Wilson B., and Ziemer, Robert R.: Investigations of Air-Cooled Turbine Rotors for Turbojet Engines. I - Experimental Disk Temperature Distribution in Modified J33 Split-Disk Rotor at Speeds up to 6000 RPM. NACA RM E51I11, 1952.

9. Smith, Gordon T., and Hickel, Robert O.: Preliminary Investigation of Hollow-Bladed Turbines Having Closed and Open Blade Tips. NACA RM E55F27a, 1955.

10. Cochran, Reeves P., and Dengler, Robert P.: Static Sea-Level Performance of an Axial-Flow Compressor Turbojet Engine with an Air-Cooled Turbine. NACA RM E54L28a, 1955.

11. Heaton, Thomas R., Slivka, William R., and Westra, Leonard F.: Cold-Air Investigation of a Turbine with Nontwisted Rotor Blades Suitable for Air Cooling. NACA RM E52A25, 1952.

12. English, Robert E., and Wachtl, William W.: Charts of Thermodynamic Properties of Air and Combustion Products from 300° to 3500° R. NACA TN 2071, 1950.

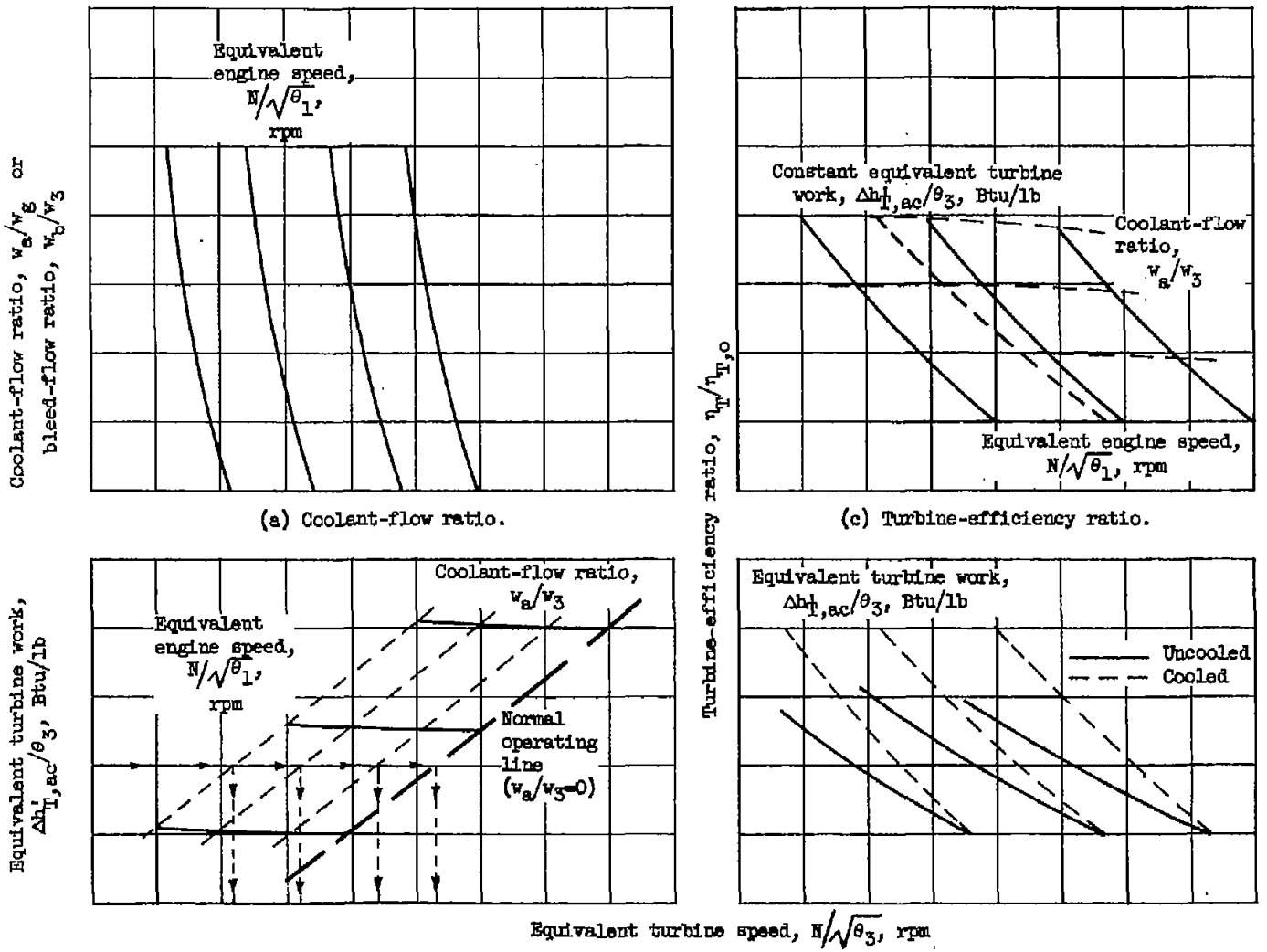

Figure 1. - General method of plotting and presenting data as function of equivalent turbine speed.

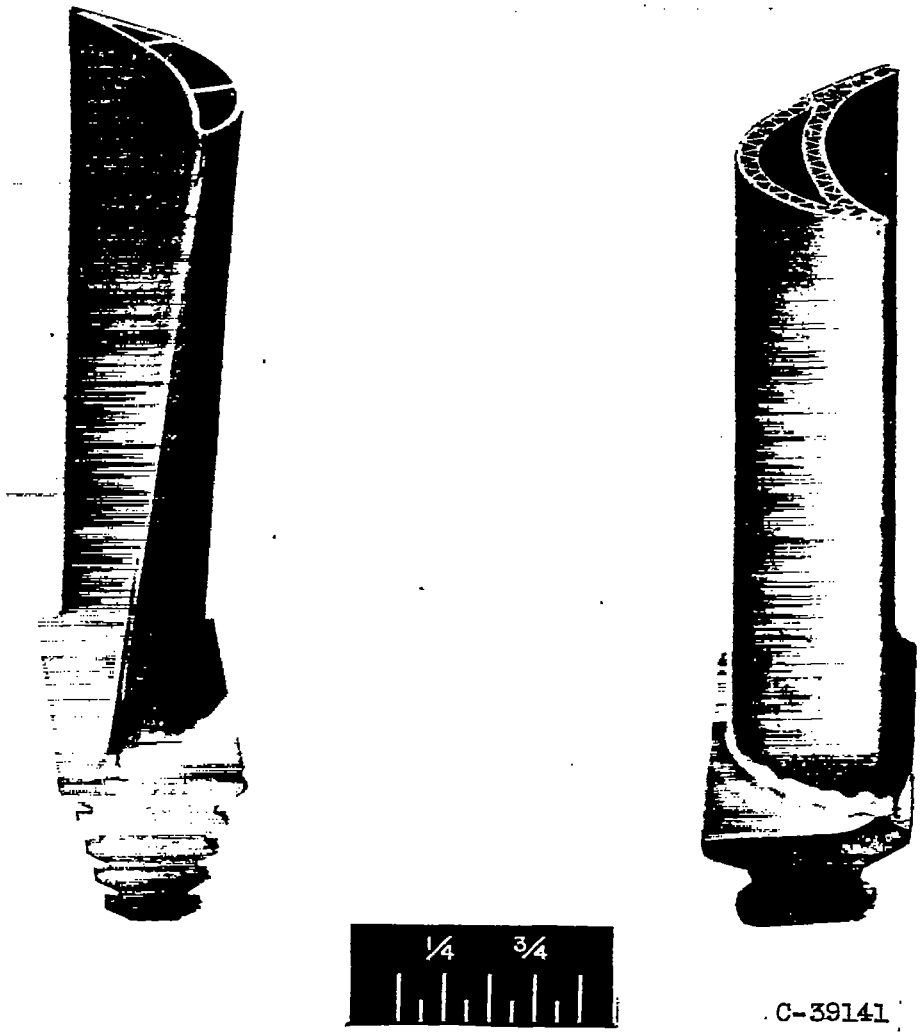

(a) Blade for turbine A. (b) Blade for turbine B.

Figure 2. - Air-cooled turbine blades used in investigation.

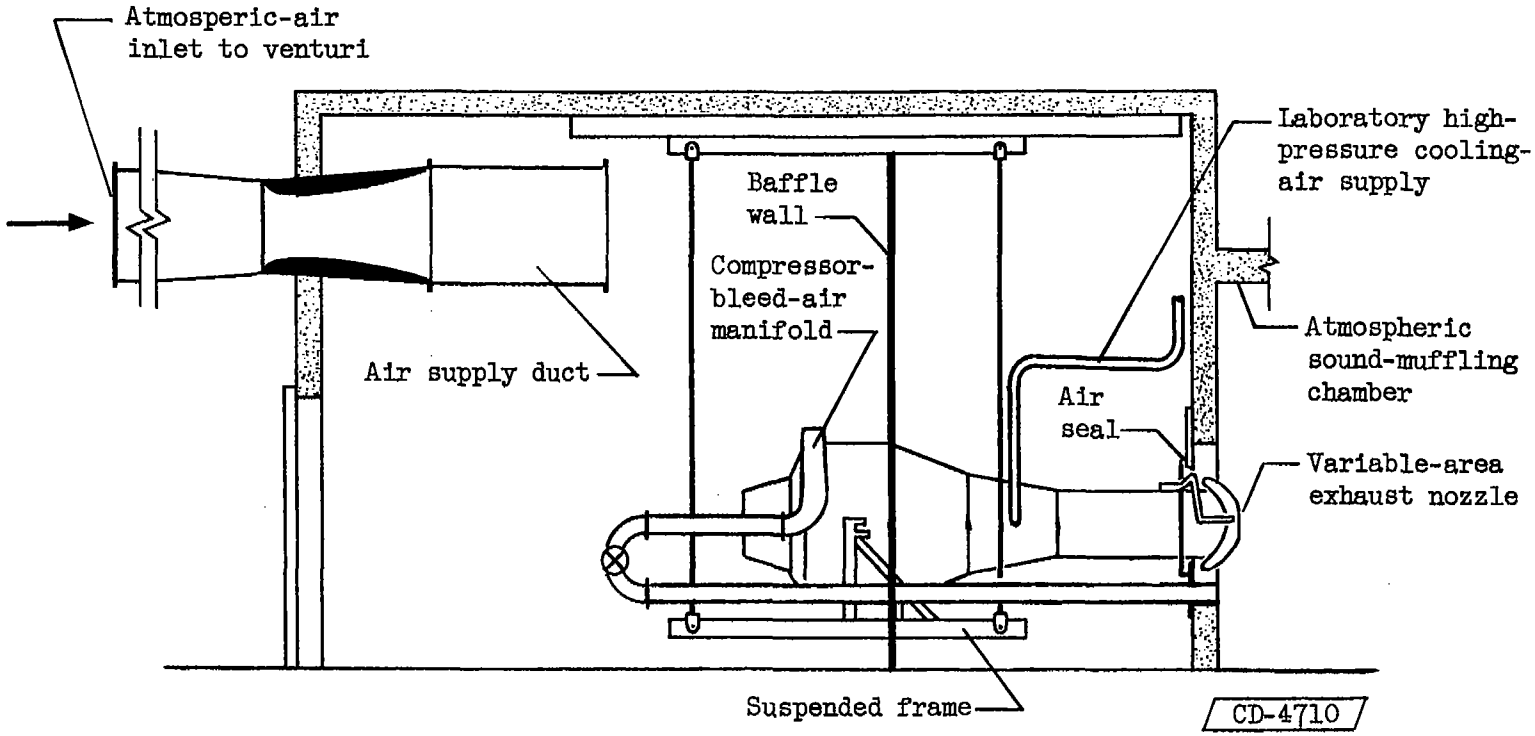

Figure 3. - Installation of centrifugal-compressor engine in test cell.

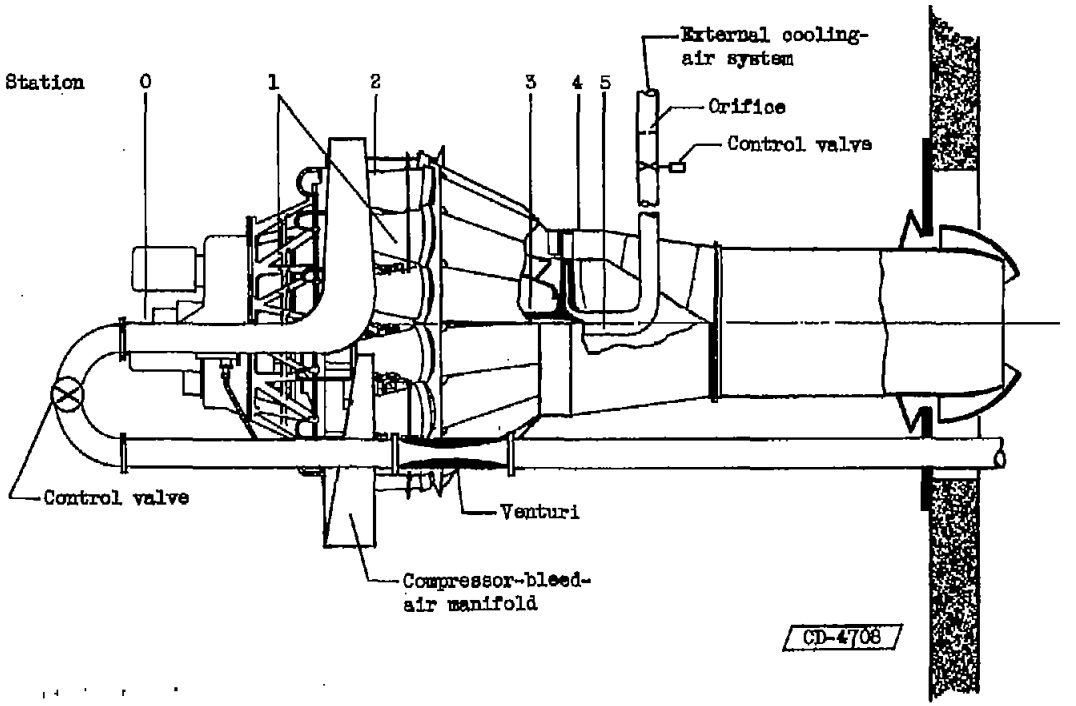

STATION 0 (cell ambient)	Station 1 (compressor inlet)	STATION 2 (compressor discharge)	STATION 3 (turbine inlet)	STATION 4 (turbine discharge)	STATION 5 (rotor cooling-air inlet)
1 Static tap in quiescent zone of cell	12 Shielded thermocouples on inlet screens, 6 front and 6 rear	Total of 8 thermocouples on 2 probes, one radial and one circumferential	7 Total-pressure measurements on 2 probes, one radial and one circumferential	Total of 36 static-pressure taps, 21 on outer shroud and 15 on inner shroud of tail cone, distributed axially and circumferentially	2 Thermocouples in sealing-air supply line at rotor hub

(a) Centrifugal-compressor engine.

Figure 4. - Type and location of instruments at instrumentation stations.

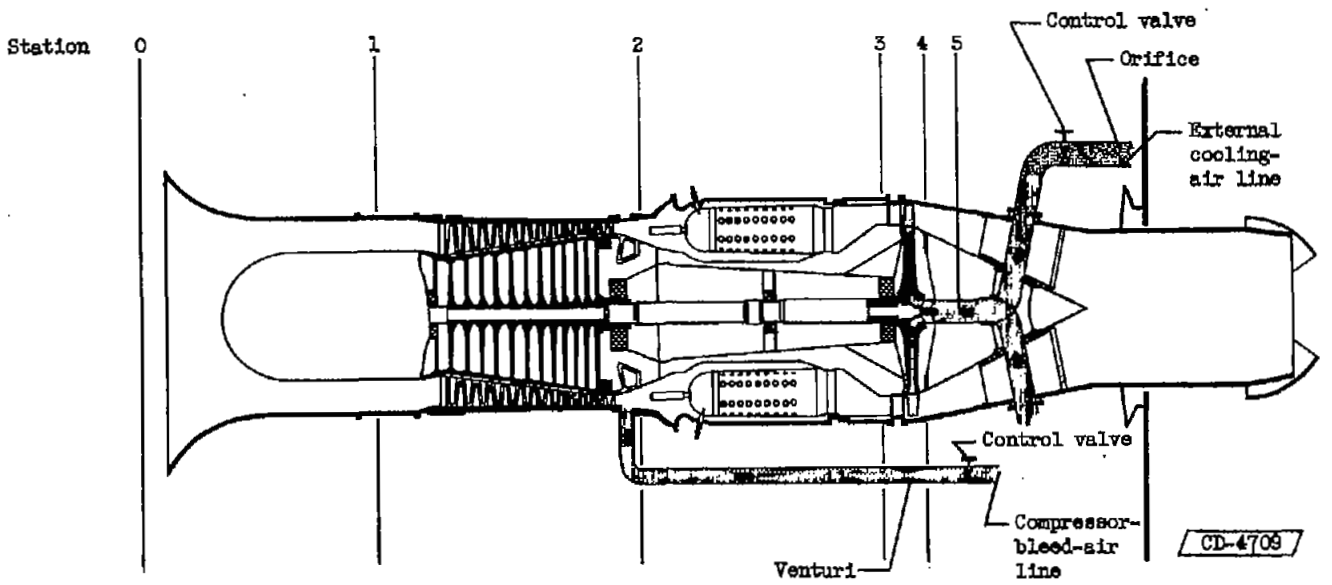

STATION 0 (cell ambient)	STATION 1 (compressor inlet)	STATION 2 (compressor outlet)	STATION 3 (turbine inlet)	STATION 4 (turbine outlet)	STATION 5 (rotor cooling-air inlet)
1 Static tap in quiescent zone of cell	14 Open-end thermocouples distributed radially and circumferentially	12 Open-end thermocouples distributed radially and circumferentially	8 Total-pressure probes; one at center of flow passage in each transition liner	39 Static-pressure taps distributed axially and circumferentially (18 on outer cone and 21 on inner cone)	1 Total-temperature probe in cooling-air supply line at rotor hub

(b) Axial-flow-compressor engine.

Figure 4. - Concluded. Type and location of instruments at instrumentation stations.

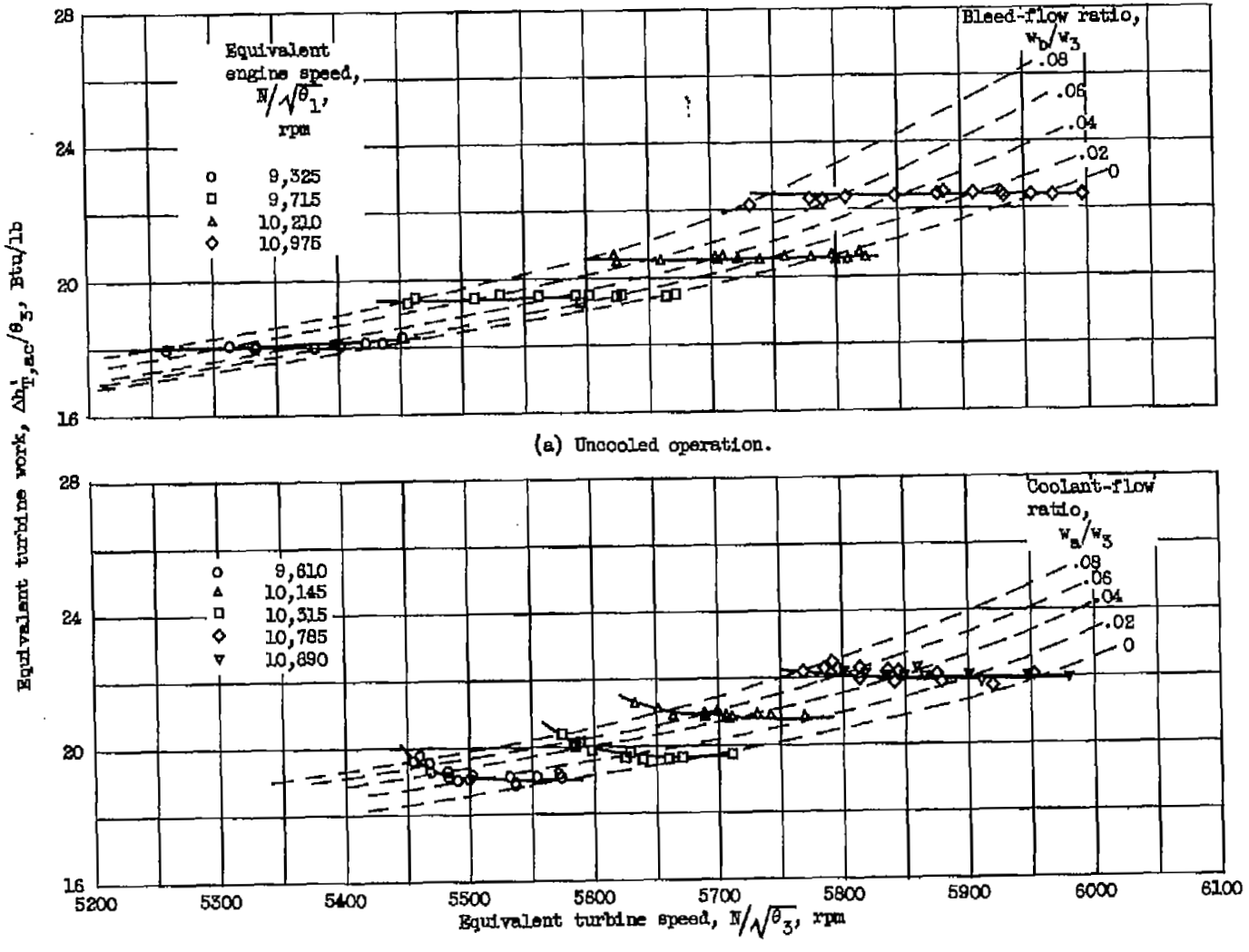

(a) Uncooled operation.

(b) Cooled operation.

Figure 5. - Variation of equivalent turbine work with equivalent turbine speed for turbine A.

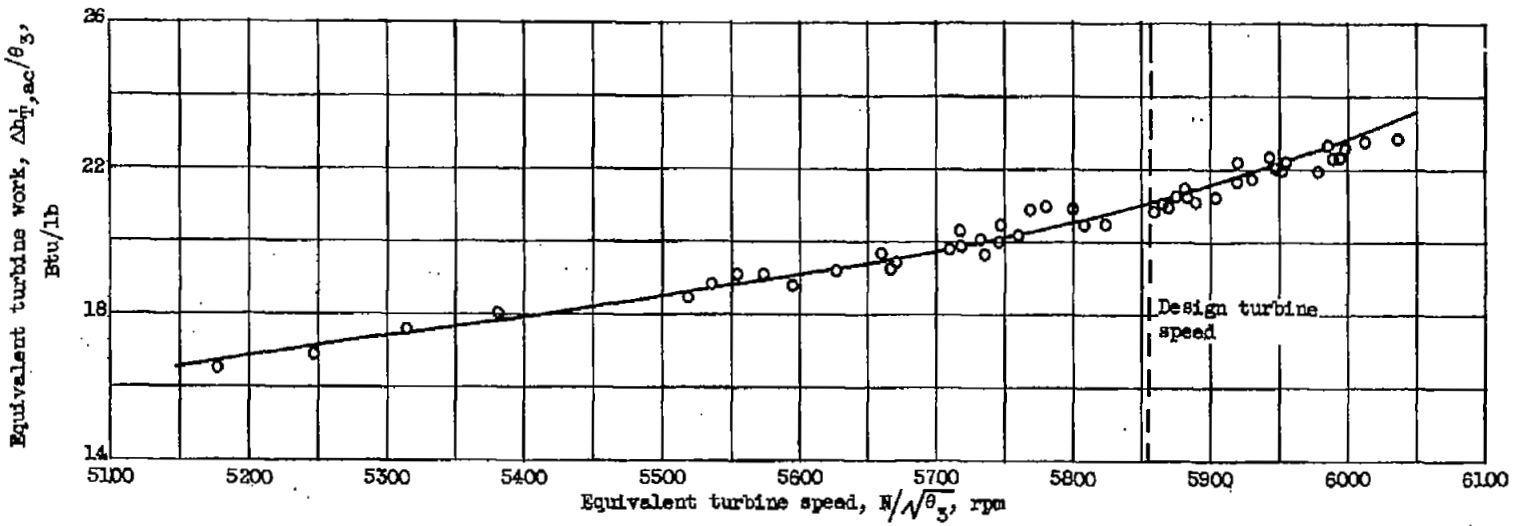

Figure 6. - Data used to establish zero compressor-bleed and zero coolant-flow rates for cross-plotting data of turbine A.

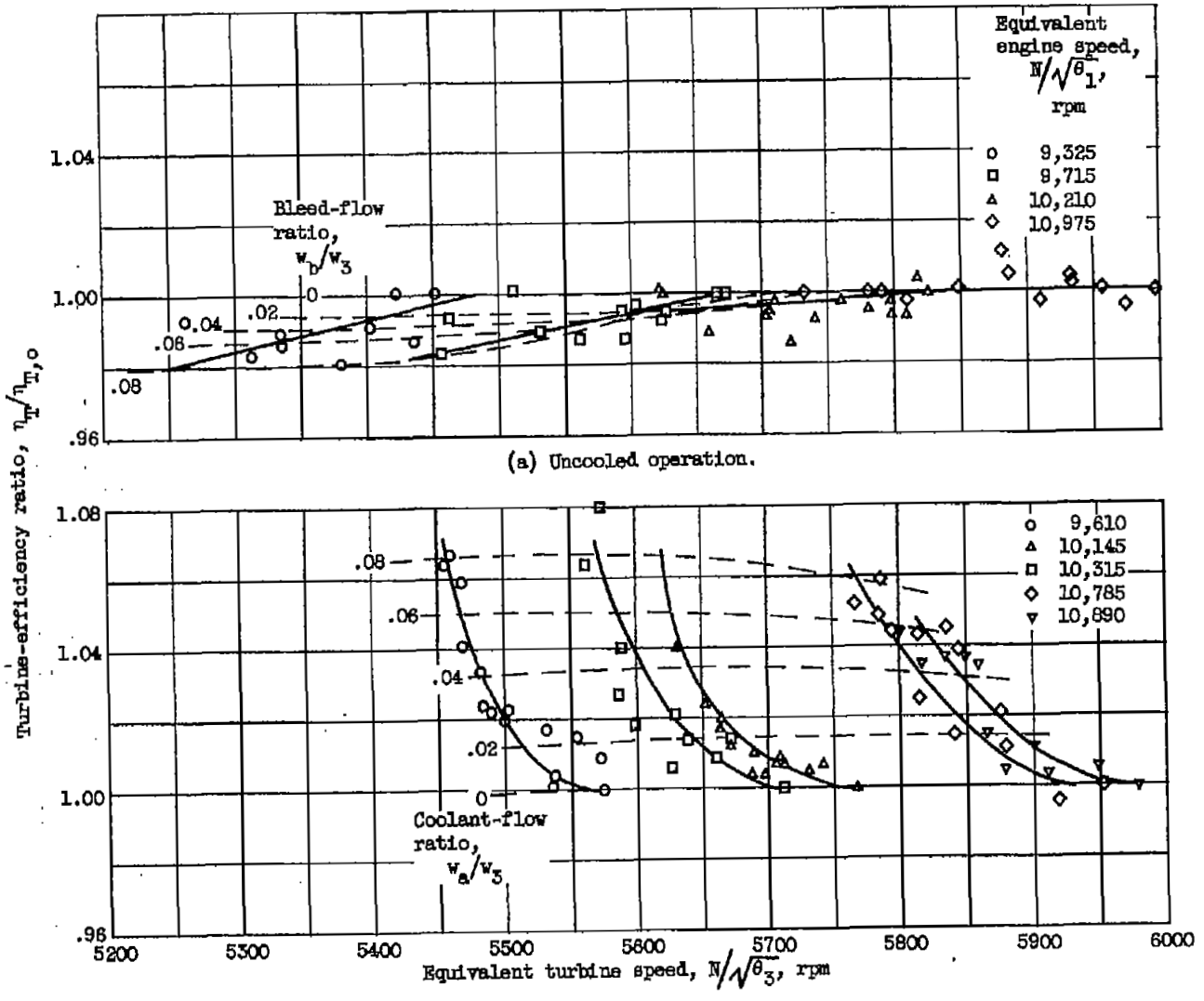

(a) Uncooled operation.

(b) Cooled operation.

Figure 7. - Variation of turbine-efficiency ratio with equivalent turbine speed of turbine A.

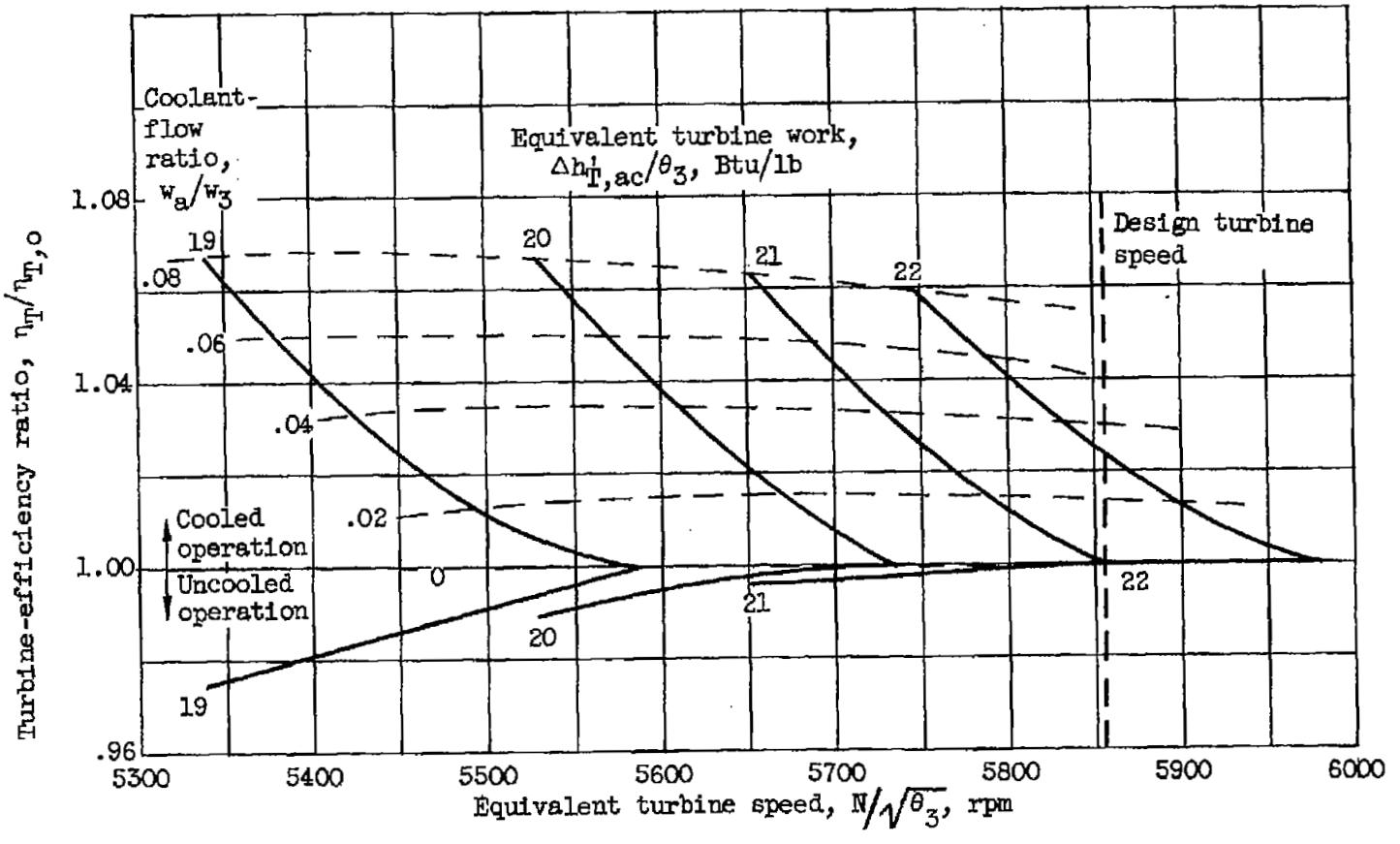

Figure 8. - Comparison of turbine-efficiency ratios obtained with turbine A.

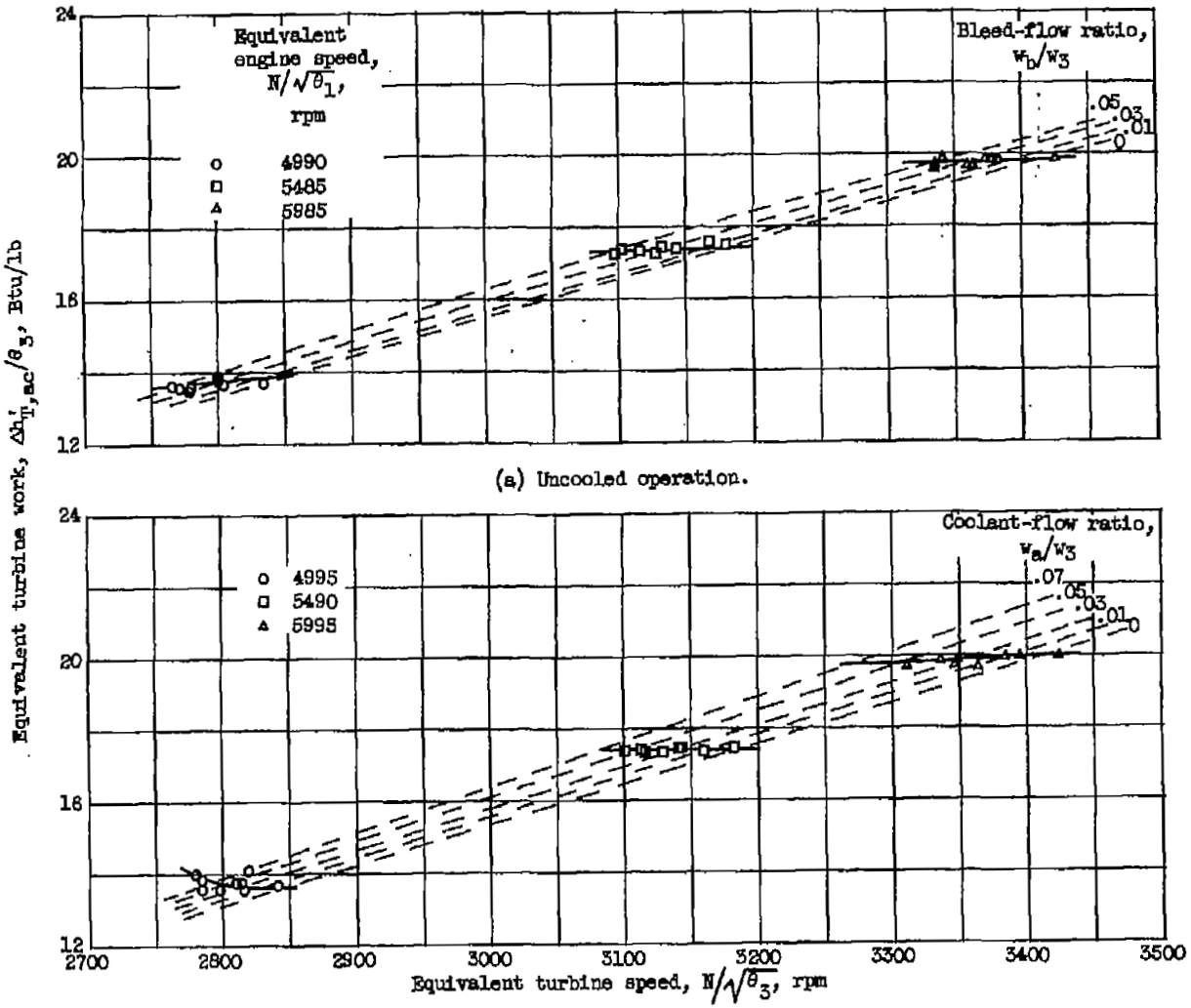

(a) Uncooled operation.

(b) Cooled operation.

Figure 9. - Variation of equivalent turbine work with equivalent turbine speed for turbine B.

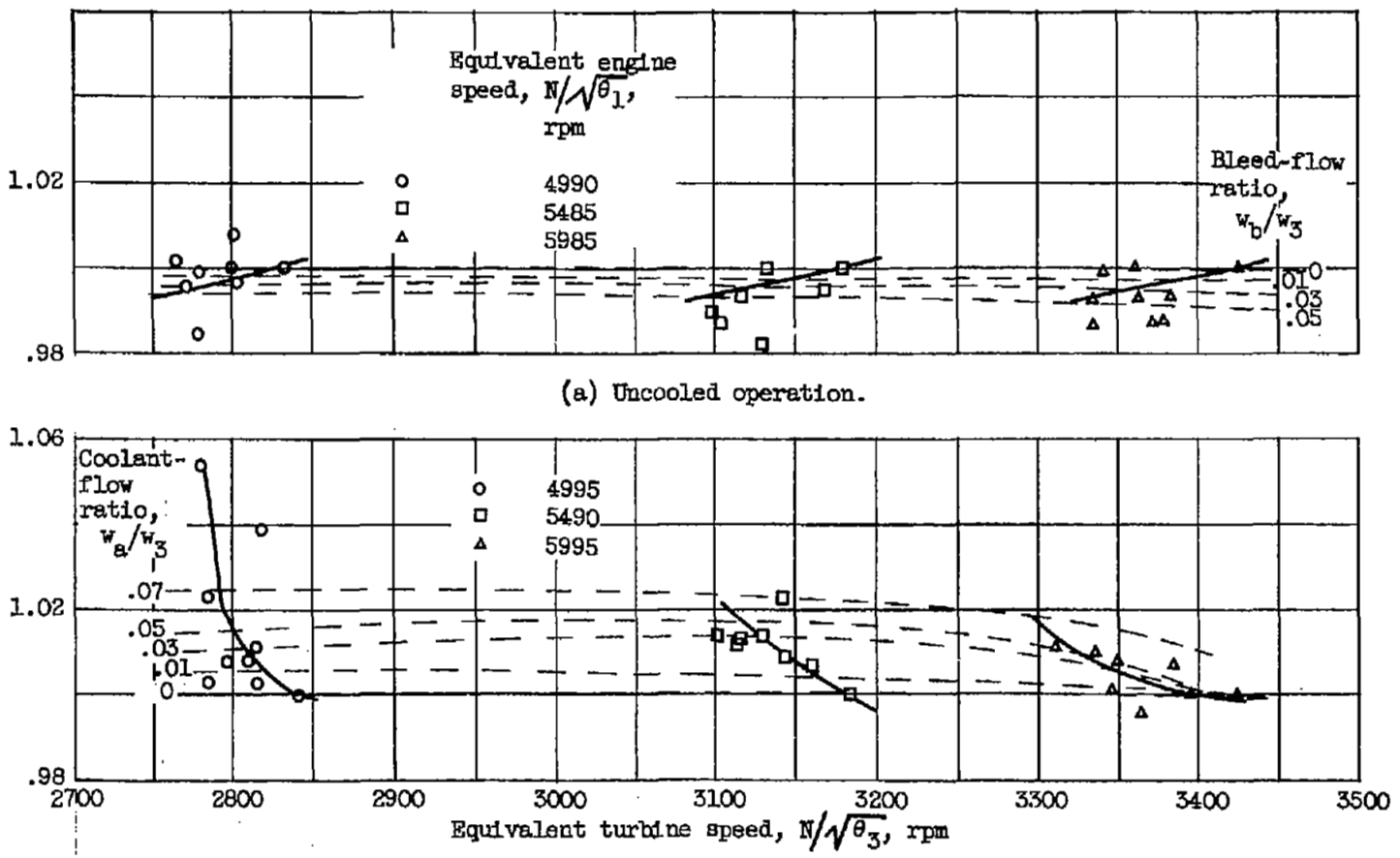

(a) Uncooled operation.

(b) Cooled operation.

Figure 10. - Variation of turbine-efficiency ratio with equivalent turbine speed of turbine B.

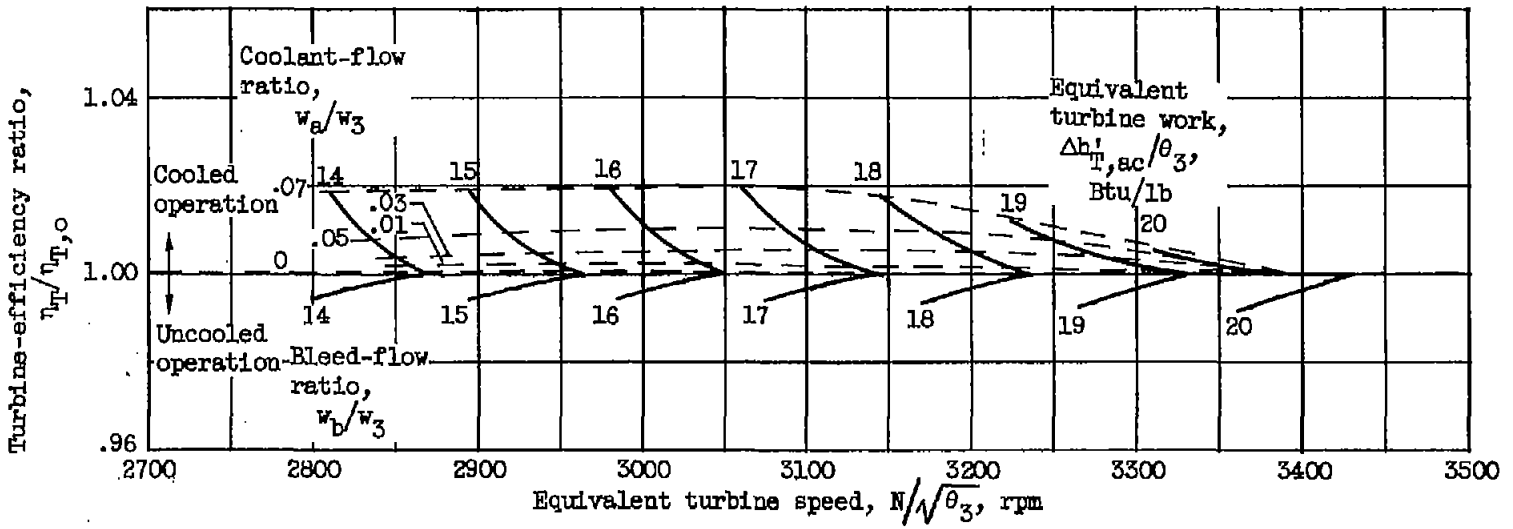

Figure 11. - Comparison of turbine-efficiency ratios obtained with turbine B.

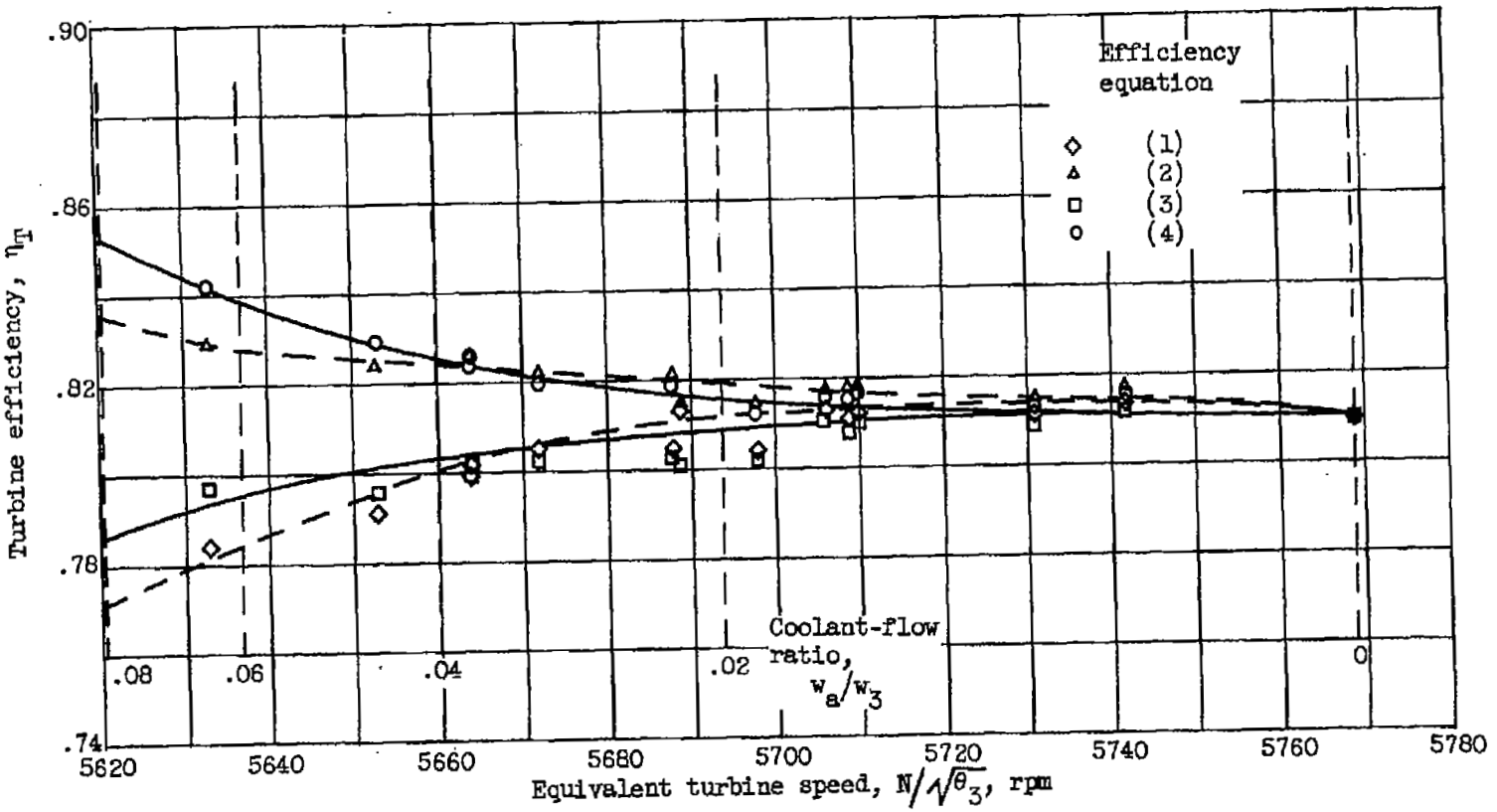

(a) Turbine A; equivalent engine speed, 10,145 rpm.

Figure 12. - Comparison of turbine efficiencies obtained by various methods.

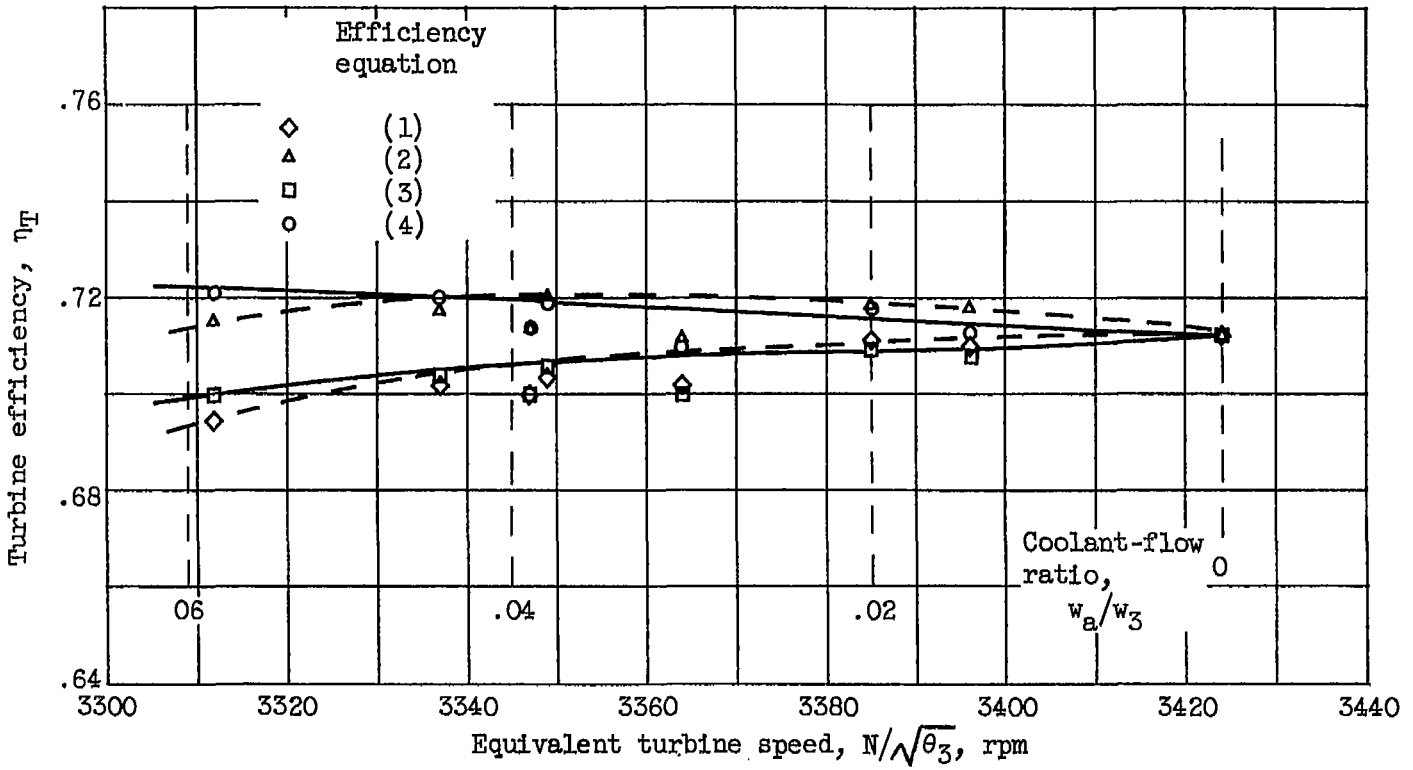

(b) Turbine B; equivalent engine speed, 5995 rpm.

Figure 12. - Concluded. Comparison of turbine efficiencies obtained by various methods.

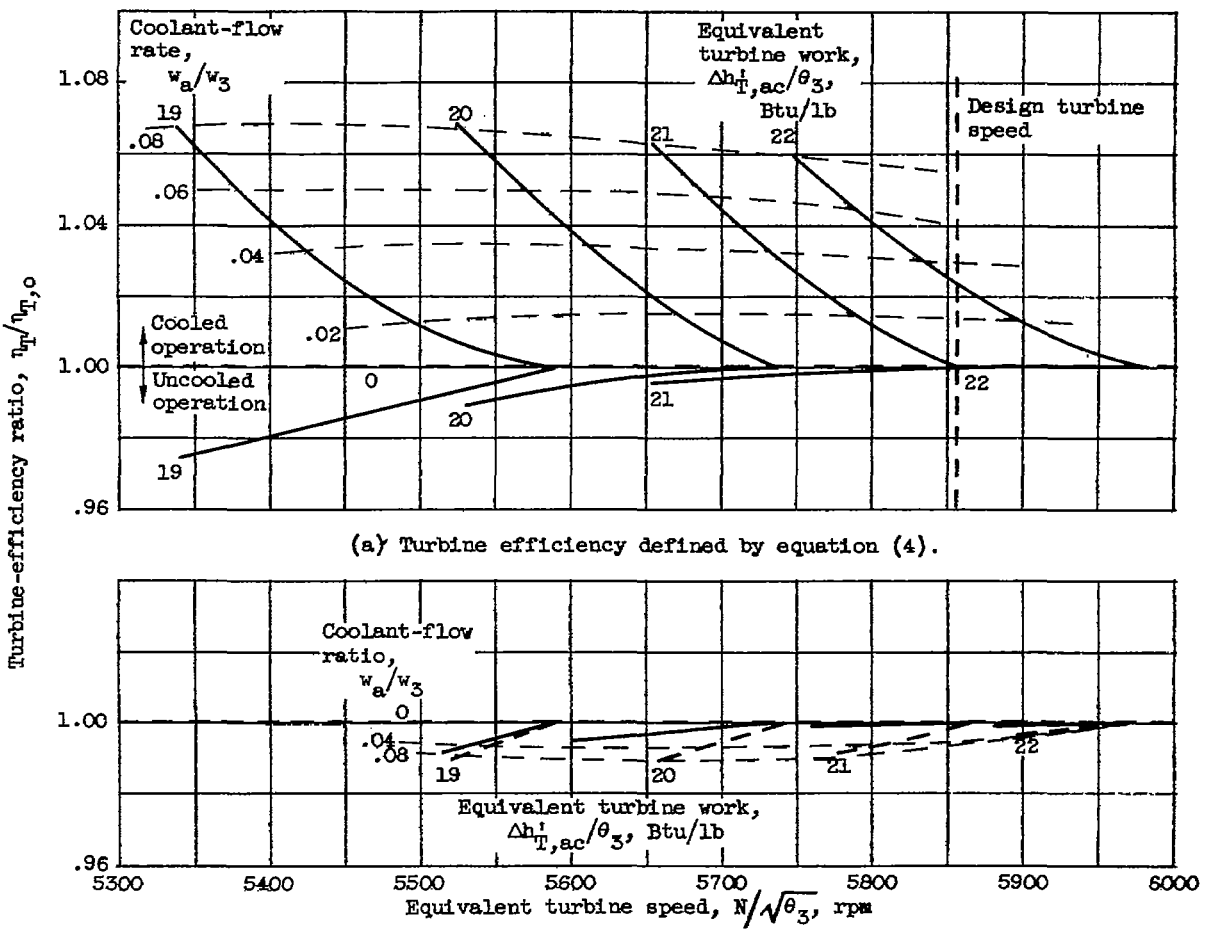

(a) Turbine efficiency defined by equation (4).

(b) Turbine efficiency defined by equation (3).

Figure 13. - Comparison of turbine-efficiency ratios obtained with turbine A over entire range of equivalent engine speeds considered.